Generation of Slow Surface Plasmon Polaritons in a Complex Waveguide Structure with Electric Current Pump

Sergey G. Moiseev,* Yuliya S. Dadoenkova, Aleksei S. Kadochkin, Andrei A. Fotiadi, Vyacheslav V. Svetukhin, and Igor O. Zolotovskii

A planar spaser structure composed of semiconducting film and graphene with DC current is proposed and theoretically explored. Graphene possesses velocity of drift current carriers comparable with the phase velocity of surface plasmon polaritons (SPPs) in ultrathin semiconducting film at the terahertz regime. When the synchronism condition between current and slow surface electromagnetic waves is realized, the amplification of plasmons by electric current takes place. In the proposed complex waveguide structure, positive feedback is realized due to reflections from the edges of the active waveguide, and the SPPs are decoupled into light by a microscopic grating manufactured on the semiconducting film surface.

1. Introduction

The problem of creating a compact source of coherent radiation based on surface plasmon polaritons (SPPs) or spasers has been the subject of many papers.[1–12] The most common spaser models are based on the principle of SPPs amplification due to the use of optical[1,3–6,8,9] or electric[2,7,10–12] pumping. The use of optical pumping is simpler in technical performance, but its implementation requires an external (macroscopic) laser, which does not allow the creation of a compact source of coherent radiation which is integrated into optoelectronic circuits.

From the point of view of on-chip spaser development, the use of electric pumping seems to be more promising. In the proposed electric spaser models, a separate active medium is added to the plasmon medium (most often structurally), providing an amplification of the SPPs. An injection spaser is proposed in ref. [2] where the amplification of SPPs propagating along the metal–semiconductor boundary occurs due to the injection of charge carriers. In ref. [12], the spaser circuit with an electric pumping is proposed, with an active element being represented by a carbon nanotube–based quantum dot, and an external resonator presented by the layers of graphene.

In refs. [13–17], a fundamentally different method of SPP amplification using an electric pumping was proposed, which does not require the presence of an additional integrated or an external active media. In this scheme, the amplification occurs as a result of direct interaction of the carriers of the drift current with the SPP wave, just as it is realized in vacuum amplifying tubes of microwave electronics (traveling wave tubes, etc.). The SSPs and pump currents are localized in carbon nanostructures (graphene layers or carbon nanotubes), which ensures efficient energy transfer to the surface wave. Here, we propose a planar design of an electric spaser, where both the SPP gain and the positive feedback are realized simultaneously as well as the far-field emission of the generated radiation. The amplification is carried out by the energy of a DC electric current passed through graphene. The resonator is performed by the active region itself, whose boundaries reflect the SPPs. The amplified SPP waves are output from the active region to the conjugate waveguide, where the far-field radiation output is realized through the diffraction grating.

The paper is organized as follows. In Section 2, we show the geometry of the plasmon waveguide structure and dispersion equation of the SPPs. In Section 3, we discuss the SPP amplification using electric current pump in graphene. In Section 4, we analyze the conditions of the SPPs generation in the plasmon waveguide and estimate the effectiveness of the diffraction grating in the transition of the SPPs into photons. Section 5 summarizes the obtained results.

Dr. S. G. Moiseev, Dr. Y. S. Dadoenkova, Dr. A. S. Kadochkin,
Dr. A. A. Fotiadi, Dr. V. V. Svetukhin, Dr. I. O. Zolotovskii
Ulyanovsk State University
Ulyanovsk 432017, Russian Federation
E-mail: serg-moiseev@yandex.ru

Dr. S. G. Moiseev
Kotelnikov Institute of Radio Engineering and
Electronics of the Russian Academy of Sciences
Ulyanovsk Branch, Ulyanovsk 432011, Russian Federation

Dr. S. G. Moiseev
Ulyanovsk State Technical University
Ulyanovsk 432027, Russian Federation

Dr. A. A. Fotiadi
Université de Mons
B7000 Mons, Belgium

Dr. V. V. Svetukhin
Institute of Nanotechnologies of Microelectronics of the Russian
Academy of Sciences
Moscow 119991, Russian Federation

**ADVANCED
SCIENCE NEWS**
www.advancedsciencenews.com
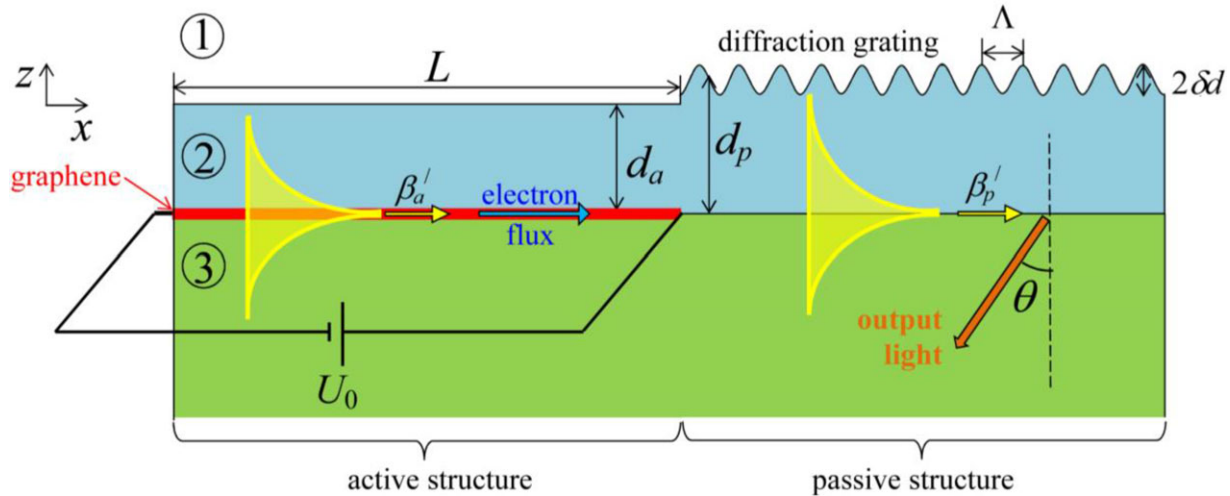
annalen
der **physik**
www.ann-phys.org

Figure 1. Schematic of the spaser with far-field radiation output of the generated SPP wave. A passive waveguide structure with the semiconducting layer thickness d_p is adjacent to an active plasmon waveguide of the length L and the semiconducting film thickness d_a with deposited graphene single layer. The radiation output of the generated SPP into the far field under an angle θ is provided by a diffraction grating (of period Λ and modulation depth δd) placed on the passive waveguide. Propagation constants of the SPP in active and passive structures are denoted β_a' and β_p', respectively. The electron flux direction under an applied voltage U_0 in the active structure is indicated by the blue arrow.

2. Geometry of Plasmon Waveguide Structure

Let us consider a structure formed by two waveguides—active and passive ones, which are composed from identical materials and have a similar configuration, as shown in **Figure 1**. These waveguides are three-layer structures composed of semi-infinite dielectric cladding "1" and substrate "3" with dielectric permittivities $\varepsilon_1 > 0$ and $\varepsilon_3 > 0$, respectively, and a semiconducting film "2" with negative real part of dielectric permittivity $\varepsilon_2 = \varepsilon_2' + i\varepsilon_2''$ ($\varepsilon_2' < 0$). The SPPs propagate along the positive direction of the x-axis with the longitudinal components of wavevectors $\beta_\eta = \beta_\eta' + i\beta_\eta''$, and the electric field components depend on time and spatial coordinates as $\tilde{E}_\eta(x, z, t) = E_\eta(x, z) \exp[i(\omega t - \beta_\eta x)]$, where the superscript $\eta = a, p$ refers to the active and passive waveguides, respectively.

Active waveguide consists of a semiconducting film of constant thickness d_a with a graphene single-layer placed on the interface between semiconducting film and substrate "3". In this waveguide, a mechanism of the slow SPP amplification is realized due to the energy of the DC current in graphene, which allows to compensate for ohmic losses in the structure.[13] A DC electric current localized in graphene is induced by an applied voltage U_0, and the direction of negative charge carriers (electrons) flux coincides with the SPP propagation direction (direction of the electron flux in graphene is shown by the blue arrow in Figure 1). The active waveguide has a finite length L ($L \gg d_a$), and its opened left-hand-side edge borders on the medium with dielectric permittivity ε_1. The dispersion equation of the SPP wave in such structure with a film with flat surfaces and with a graphene sheet has the form[18]

$$\exp(-2q_{a2}d_a) = \frac{q_{a2}\varepsilon_1 + q_{a1}\varepsilon_2}{q_{a2}\varepsilon_1 - q_{a1}\varepsilon_2} \cdot \frac{q_{a2}\varepsilon_3 + q_{a3}\varepsilon_2 + i4\pi q_{a2}q_{a3}\sigma/\omega}{q_{a2}\varepsilon_3 - q_{a3}\varepsilon_2 + i4\pi q_{a2}q_{a3}\sigma/\omega}$$

(1)

where $q_{aj} = \sqrt{\beta_a^2 - k_0^2\varepsilon_j}$ is the transverse component of the SPP wavevector in medium with dielectric permittivity ε_j ($j = 1, 2, 3$), σ is the graphene surface conductivity, $k_0 = \omega/c$ and c are the wavevector and speed of light in vacuum, respectively.

The waveguide structure which is adjacent to the active waveguide on the right-hand side contains a semiconducting film of thickness d_p. We consider the case when the thicknesses of semiconducting film in the active and passive waveguides are similar ($d_p/d_a \approx 1$), which reduces the scattering of the SPP at the interface between the waveguides. A diffraction grating with period Λ and small modulation depth $\delta d \ll d_p$ is placed on the top surface of the semiconducting film to provide the transition of SPPs into photons emitted into substrate. As is known, the presence of a grating leads to a difference between the characteristics of the SPP and those of a structure with flat surfaces, including changes in the propagation constant and increase in the damping due to radiation losses.[19,20] However, since the modulation depth of the grating is much less than both the film thickness and the wavelength of the SPP, and as a consequence, the influence of the grating gives a small effect, the characteristics of the SPP in the passive waveguide with corrugation are sufficiently well described, in the first approximation, by the dispersion relation for a film with flat surfaces.

$$\exp(-2q_{p2}d_p) \approx \frac{q_{p2}\varepsilon_1 + q_{p1}\varepsilon_2}{q_{p2}\varepsilon_1 - q_{p1}\varepsilon_2} \cdot \frac{q_{p2}\varepsilon_3 + q_{p3}\varepsilon_2}{q_{p2}\varepsilon_3 - q_{p3}\varepsilon_2}$$

(2)

where $q_{pj} = \sqrt{\beta_p^2 - k_0^2\varepsilon_j}$ ($j = 1, 2, 3$).

In fact, the structure shown in Figure 1 is an analog of the Fabry–Pérot interferometer in which resonator is represented by an active waveguide. Positive feedback, which is necessary for establishing the generation mode, is realized by reflection of the amplified SPP wave from the boundaries of the active waveguide.

The generation condition for the SPP in the active structure and the conditions for matching the radiation characteristics and the parameters of the diffraction grating for the emission of radiation from the passive waveguide structure will be considered in Section 4.

3. Amplification of Surface Plasmon Polariton Wave in Active Waveguide Structure

In this section, we perform a brief analysis of the SPP amplification in active waveguide structure with drift current pumping. As was shown in refs. [13,14,16,17], on the basis of known equations of microwave technology[21,22] one can obtain a system of equations, which describes the interaction of the field of SPP wave and electric current pump in the following form.

$$\frac{dE_a}{dx} + i\frac{\omega}{V_a}E_a = -\frac{1}{2}\frac{\omega^2}{V_a^2}K\,I \quad (3a)$$

$$\frac{d^2}{dx^2}\Delta I + 2i\frac{\omega}{V_0}\frac{d}{dx}\Delta I - \frac{\omega^2-\omega_q^2}{V_0^2}\Delta I = i\frac{\omega}{V_0}\frac{I_0}{2U_0}E_a \quad (3b)$$

where E_a and $V_a = \omega/\beta_a'$ are the longitudinal field component (x-component) and the phase velocity of the SPP wave in active structure, V_0 is the drift velocity of the charge carriers, ω_q is reduced plasma frequency, K is the coupling parameter, which describes the interaction efficiency between the current and generating surface electromagnetic waves (see details in refs. [13,17]). Note that Equation (3b) is obtained for small perturbations of the current amplitude: $\Delta I(x) = (I(x) - I_0) << I_0$, where I_0 is an amplitude-constant current flowing in the absence of perturbation caused by SPP wave.

Assuming that the perturbations of drift current and SPP wave field are changing along the waveguide proportionally to $\exp(-iGx)$, where G is the complex growth rate of the harmonic disturbance, one can obtain the following dispersion relation from Equation (3).

$$(\omega - GV_a)\left[(\omega - GV_0)^2 - \omega_q^2\right] = C^3\omega^3 \quad (4)$$

where the parameter $C = (KI_0V_0^2/4U_0V_a^2)^{1/3}$ is analogous to the Pierce gain parameter used in microwave technology.[23] The complex roots of Equation (4) give the value of the SPP amplification coefficient α as

$$\alpha = \mathrm{Im}(G) > 0 \quad (5)$$

Figure 2 presents the frequency dependences of the SPP propagation constant, phase and group velocities, and amplification coefficient in the active waveguide structure. The dielectric permittivities of the cladding and substrate are $\varepsilon_1 = 1$, $\varepsilon_3 = 3$, respectively. The dielectric permittivity of the semiconducting film $\varepsilon_2(\omega)$ is taken for PbS,[24] and its thickness is $d_a = 0.1\,\mu\mathrm{m}$. The graphene surface conductivity in the terahertz regime is calculated using the expression which takes into account the loss in
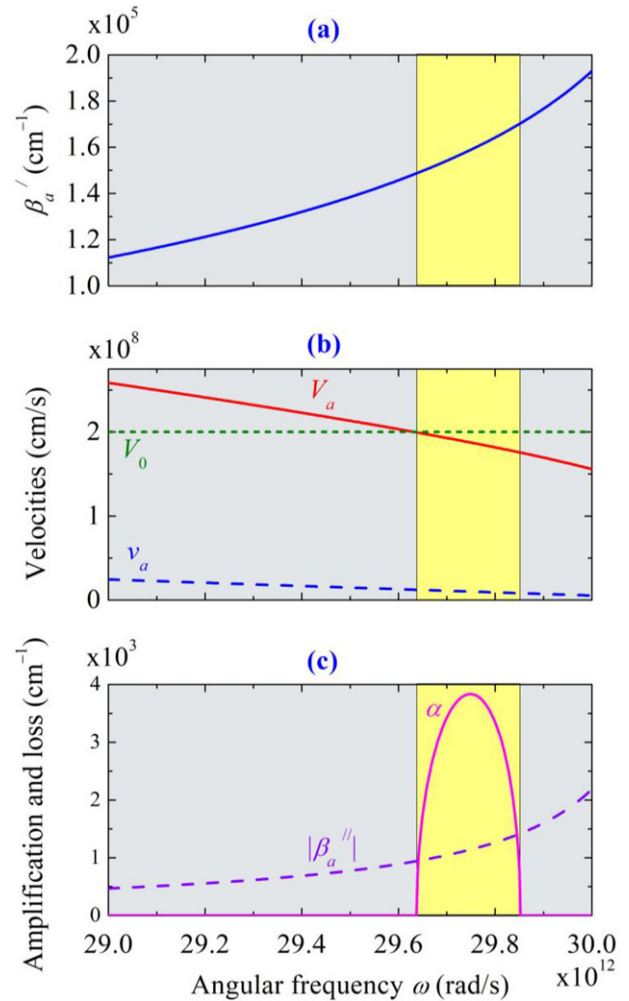

Figure 2. Frequency dispersion of the SPP parameters for the active structure (see Figure 1): a) propagation constant β_a'; b) phase velocity V_a (solid red line), group velocity v_a (dashed blue line), and drift current velocity V_0 (dotted green line); c) amplification coefficient α (solid magenta line) and absolute value of loss coefficient $|\beta_a''|$ (dashed violet line). Parameters of the structure are given in the text. The yellow areas show the frequency interval of the amplification band.

graphene.[25,26]

$$\sigma(\omega, \mu_c, \Gamma, T) = \frac{ie^2(\omega + i2\Gamma)}{\pi\hbar}$$

$$\times \left[\int_0^\infty \frac{f_d(-\omega) - f_d(\omega)}{(\omega + i2\Gamma)^2 - 4\omega^2}d\omega - \frac{1}{(\omega + i2\Gamma)^2}\int_{-\infty}^\infty \frac{\partial f_d(\omega)}{\partial\omega}|\omega|\,d\omega\right]$$

$$(6)$$

where e is electron charge, $f_d = \{\exp[(\hbar\omega - \mu_c)/k_B T] + 1\}^{-1}$ is the Fermi–Dirac distribution, μ_c is chemical potential, T is temperature, Γ is a phenomenological scattering rate, $\hbar$ is the reduced Planck constant, and k_B is Boltzmann constant. In our calculations, we assume $T = 300\,\mathrm{K}$, $\mu_c = 0.2\,\mathrm{eV}$, and $\Gamma = 1\,\mathrm{meV}$.

**ADVANCED
SCIENCE NEWS**

www.advancedsciencenews.com

annalen
der **physik**

www.ann-phys.org

As one can see from Figure 2a, the values of the SPP propagation constant $\beta_a' \approx 10^5 \, \text{cm}^{-1}$ are two orders of magnitude larger than the values of $k_0 \approx 10^3 \, \text{cm}^{-1}$ in the considered frequency range. In this case, the SPP is indeed slow: $V_a \approx (1.5-2.5) \times 10^8 \, \text{cm s}^{-1}$ (see Figure 2b), which is approximately two orders of magnitude less than the propagation velocity of electromagnetic waves in bulk media. Such slow surface waves which satisfy the synchronism condition (SPP phase velocity V_a should be comparable to but less than the drift velocity V_0 of charge carriers) can be amplified by a flux of charged particles in graphene. Due to large mobility of the charges in graphene the response strength of the charge carriers to an applied electric field is high, which provides an effective interaction of drift current and SPP wave.[13,17]

As is known, the charges in graphene move with drift velocity $V_0 \approx V_F$, where V_F is Fermi velocity.[27] Here, for the numerical analysis of the regimes of amplification and generation of SPPs, the velocity of current carriers in graphene is chosen to be $V_0 = 2 \times 10^8 \, \text{cm s}^{-1}$. Such charge velocity is larger than the standard Fermi velocity in graphene $V_F \approx (0.1-1) \times 10^8 \, \text{cm s}^{-1}$.[28–30] But it should be noted that at present the efforts for fabrication of composite graphene structures with large Fermi velocities are in progress. Such techniques are called "Fermi velocity engineering."[31,32] The experimental results indicate the actual fabrication of structures with the Fermi velocity up to $(1.1-3) \times 10^8 \, \text{cm s}^{-1}$.[33–35] The use of graphene composites with a high carrier velocity will be extremely convenient for fabrication of tunable oscillators operating in a wide frequency range (from THz to UV inclusively). On the other hand, all the regimes of amplification and generation of SPPs in the structure considered here can also be implemented in the case of smaller values of the drift velocity of the current carriers down to $10^8 \, \text{cm s}^{-1}$. The only difference is that in order to obtain the same values of the amplification coefficients in the same spectral range at smaller values of the drift velocity will require the use of thinner semiconducting films.

Comparison of the SPP amplification coefficient α and ohmic loss coefficient $|\beta_a''|$ is shown in Figure 2c. One can see that for the considered structure the amplification can be higher than the ohmic loss ($\alpha > |\beta_a''|$). The amplification band width is about $\Delta\omega_a \approx 0.22 \times 10^{12} \, \text{rad s}^{-1}$, as shown with the yellow area in Figure 2. The SPP amplification coefficient reaches maximum with $\alpha_{\max} \approx 4 \times 10^3 \, \text{cm}^{-1}$ at the center of the amplification band. Note that $\alpha_{\max}$ is almost three times larger than the loss coefficient $|\beta_a''|$.

4. Generation of Surface Plasmon Polaritons in a Planar Structure with Drift Current Pump

Active waveguide structure shown in Figure 1 is limited along the x-axis by two interfaces where the amplified running SPP wave undergoes reflections. The left-hand-side interface is an opened edge of the planar structure which borders on a medium with dielectric permittivity ε_1. The right-hand-side interface is formed by a contact with a passive waveguide structure. As a result of re-reflections from these interfaces, standing SPP waves are formed in the active structure. In this case, the considered structure is similar to a Fabry–Pérot microresonator.

The SPP generation condition is determined by the condition for reproducing the complex wave amplitude when the resonator region is completely traversed. Taking into account that in the considered structure the amplification is realized in one direction only (along the x-axis), the generation condition has the form[36]

$$r_a r_{a-p} \exp\left[\left(\alpha - 2\,|\beta_a''|\right) L\right] \exp\left[2i\beta_a' L\right] = \exp\left[2i\pi m\right] \tag{7}$$

where m is integer, r_a is the reflection coefficient of the wave at the opened end, r_{a-p} is the reflection coefficient at the interface with the passive structure, and L is the active waveguide length. The values of these reflection coefficients can be found using Fresnel relations.[37]

At the left-hand-side edge of the active structure, the slow SPP waves (with an aspect ratio $V_a/c << 1$) undergo a strong reflection. Indeed, for $\beta_a' >> \{k_0\sqrt{\varepsilon_1}, |\beta_a''|\}$ the Fresnel reflection coefficient

$$r_a = \frac{\beta_a' + i\beta_a'' - k_0\sqrt{\varepsilon_1}}{\beta_a' + i\beta_a'' + k_0\sqrt{\varepsilon_1}} \approx 1 - 2\frac{k_0}{\beta_a'}\sqrt{\varepsilon_1} \tag{8}$$

is approximately equal to unity.

The active and passive parts of the waveguide structure are distinguished by the thickness of the semiconducting film, in addition, there is no graphene in the passive region. This leads to a difference in the propagation constants β_a and β_p, which one can see from **Figure 3**. Taking into account the dispersion equations, Equations (1) and (2), for slow SPPs (β_a', $\beta_b' >> k_0$) the reflection coefficient at this interface can be written as

$$r_{a-p} \approx \frac{\beta_a' - \beta_p'}{\beta_a' + \beta_p'} \approx \frac{d_p - d_a}{d_p + d_a} \tag{9}$$

Taking into account the expressions given above for slow SPP waves, the generation condition can be written in the following form.

$$\beta_a' L = \pi\,|m| \tag{10a}$$

$$\frac{|d_a - d_p|}{d_a + d_p} \exp\left[\left(\alpha - 2\,|\beta_a''|\right) L\right] \approx 1 \tag{10b}$$

Note that Equation (10a) imposes a restriction on the minimum length of the active region: $L \geq \pi/\beta_a'$. Using the results of the calculations shown in Figure 2a, one can find that under the conditions of slow SPPs amplification the length of the active region must be at least $\pi/(1.7 \times 10^5 \, \text{cm}^{-1}) \approx 0.185 \, \mu\text{m}$.

The angular frequencies of the generated SPP wave calculated according to Equations (10a) and (10b) are presented in **Figure 4**a,4b, respectively, as functions of the active waveguide length L and the ratio d_p/d_a between the semiconducting film thicknesses in the passive and active waveguides. These dependencies are shown with the set of lines corresponding to $m = 120, 130, 140$.

From Figure 4b one can see that in some intervals of the ratio d_p/d_a the SPP generation does not take place (for instance, for $0.91 < d_p/d_a < 1.1$ at $m = 120$ and $0.94 < d_p/d_a < 1.07$ at $m = 140$—see the inset in Figure 4b) because no frequencies satisfy Equation (10b). The larger the m is, the narrower the
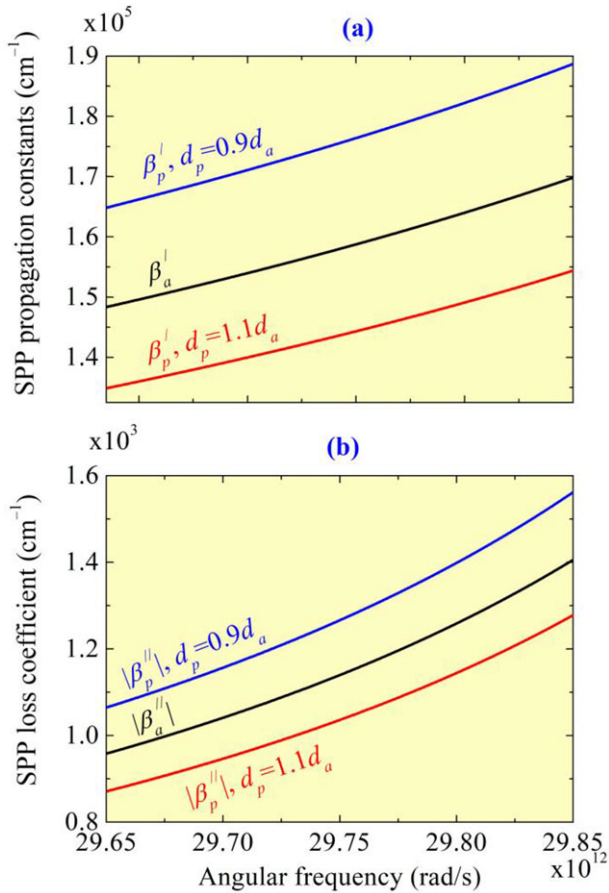
**ADVANCED
SCIENCE NEWS**

www.advancedsciencenews.com

annalen
der **physik**

www.ann-phys.org

Figure 3. a,b) Frequency dispersion of the propagation constants β'_a and β'_p, (a), and loss coefficients β''_a and β''_p (b) of SSPs in active and passive waveguide structures. Thicknesses of semiconducting films are: in active structure $d_a = 0.1 \, \mu m$ (black line), and in passive structure $d_p = 0.9 \, d_a$ (blue line) and $d_p = 1.1 \, d_a$ (red line). Other parameters are the same as in Figure 2. The frequency interval corresponds to the amplification band.

Figure 4. a,b) Generation frequency ω as function of the active waveguide length L (a) and the ratio d_p/d_a of the semiconducting film thicknesses in the passive and active waveguides (b). Parameters of the structure are the same as in Figure 2, and the set of curves are obtained for $m = 120$, 130, and 140 (solid red, dashed green, and dotted blue lines, respectively). The frequency range in (a) corresponds to the amplification band, and green shaded area corresponds to the frequency interval shown in (b). Zoom of the white area in (b) is shown in the inset.

forbidden interval in d_p/d_a is. Beyond these intervals, for each value of d_p/d_a and each m Equation (10b) has two solutions corresponding to two frequencies. However, this fact does not lead to the possibility of SPP generation at two frequencies simultaneously, since according to Figure 4a these solutions correspond to different active waveguide lengths L.

For the fixed values of the microresonator length L and the ratio d_p/d_a between the film thicknesses in the passive and active waveguides, the generation of the SPP waves will be possible at the frequency which corresponds to some integer m in Equation (10a). The SPP generator having a fixed active region length and a predetermined generation frequency can be constructed for two values of d_p/d_a: the first one for $d_p/d_a < 1$ and the second one for $d_p/d_a > 1$. For instance, in order to obtain the SPP generation at frequency $29.75 \times 10^{12} \, rad \, s^{-1}$ in the structure with the active waveguide length $L = 19 \, \mu m$ (which corresponds to $m = 120$), the thickness of the semiconducting film in the passive waveguide should be either $d_p = 0.9 d_a$ or $d_p = 1.11 d_a$ for $d_a = 0.1 \, \mu m$. It should be noted that the branches of Equation (10b) solutions are non-symmetric with respect to the vertical axis
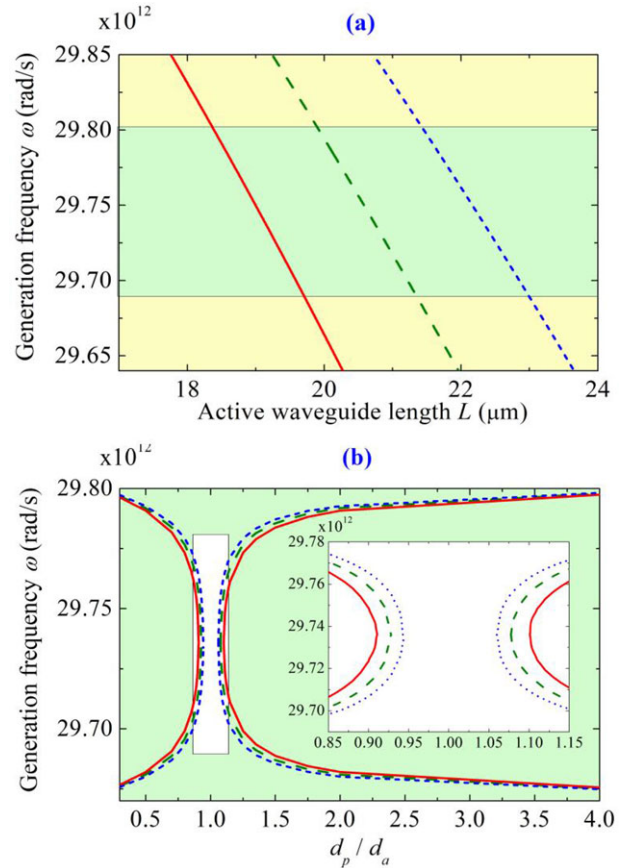
in Figure 4b due to the frequency dispersion of the longitudinal component of SPP wavevectors β_a and β_p in the active and passive waveguides (see Figure 3).

From the dependencies presented in Figure 4, it follows that by varying the structural parameters of the waveguide system it is possible to adjust the generation frequency within the SPP amplification band. It is worthy to note that the band of the allowed frequencies ($29.68 \times 10^{12} \, rad \, s^{-1} < \omega < 29.80 \times 10^{12} \, rad \, s^{-1}$, see Figure 4b) is less than the amplification band ($29.64 \times 10^{12} \, rad \, s^{-1} < \omega < 29.85 \times 10^{12} \, rad \, s^{-1}$, see Figure 2c) due to absorption in the waveguide.

The amplified SPP waves penetrate into the passive waveguide through the interface between the active and passive structures. In the latter, the radiation output to the far field is realized via the diffraction grating. Without lack of generality, let us consider the case when radiation is output to a substrate, and the phase-matching condition

$$\left| \beta'_p - 2\pi l/\Lambda \right| = k_0 \sqrt{\varepsilon_3} \sin \theta \qquad (11)$$

is fulfilled, where θ is the angle of emission (as shown at Figure 1). Here we consider the first diffraction order ($l = 1$) on the grating with period Λ satisfying the relation ($\beta_p' - 2\pi/\Lambda$) < 0.

Due to the high localization of the slow SPP wave on the interfaces and under the phase-matching condition Equation (11), the SPP mode effectively interacts with the emitted wave. In this case, in order to estimate the effectiveness of the grating in the transition of the SPPs into photons, one can use the method developed in the theory of coupled modes.[36] According to this approach, the dynamics of the SPP mode and the emitted wave is described by the following system of equations.

$$\frac{\partial A_p}{\partial x} = i\kappa A_{\mathrm{rad}} - \left|\beta_p''\right| A_p,$$
$$\frac{\partial A_{\mathrm{rad}}}{\partial x} = -i\kappa A_p + \left|\beta_p''\right| A_{\mathrm{rad}} \qquad (12)$$

where A_p is an amplitude of the SPP in the passive waveguide, A_{rad} is an amplitude of the emitted wave, and $\kappa \approx \beta_p' \delta d/2d_p$ is the parameter characterizing the relation between the SPP and the emitted waves. The solution of the system of equations, Equation (12), makes it possible to obtain approximate expressions for the mean free path length for radiation loss

$$\xi_{\mathrm{rad}} \approx \frac{2}{\kappa} \approx \frac{4}{\beta_p'} \frac{d_p}{\delta d} \qquad (13)$$

and the efficiency of grating

$$\eta \approx \exp\left[-2\beta_p'' \xi_{\mathrm{rad}}\right] \approx \exp\left[-8\frac{\beta_p''}{\beta_p'} \frac{d_p}{\delta d}\right] \qquad (14)$$

calculated as the ratio of the power flow of the emitted wave to the power flow of the SPP wave at the input to the grating. For the propagation constant $\beta_p' \approx \beta_a' \approx 1.6 \times 10^5$ cm^{-1} (see Figure 4), the length of the radiation loss ξ_{rad} takes values in the range approximately from 2.5 to 25 μm (for $0.01 < \delta d/d_p < 0.1$), which is less or comparable to the value of the SPP propagation length $\xi_p = 1/\beta_p'' \approx 10$ μm. Since the grating period is $\Lambda \approx 2\pi/\beta_p' \approx 0.4$ μm, at the total mean free path length, given by $\xi = (\xi_{\mathrm{rad}}^{-1} + \xi_p^{-1})^{-1}$, there are 5−18 grating periods. The efficiency η, calculated using Equation (14), takes values from tenths of a percent to several tens of a percent (up to 60%). The obtained values of the grating efficiency are in a good agreement with the results of the experimental studies and numerical simulations.[38–40]

5. Conclusion

We propose a plasmonic laser (spaser) structure, in which the conversion of the localized SPP waves into uncoupled light is realized. The amplification of SPPs is provided directly by the flow of charge carriers that form a DC current in graphene placed on a semiconducting film. Feedback is realized due to reflections of the surface waves from the boundaries of an active waveguide. The radiation output of the generated SPP waves into the far field is realized using an adjacent passive waveguide similar to the active one except without graphene layer, but with diffraction grating manufactured on top of the semiconducting film. We analyze

the generation condition depending on the geometry parameters of the waveguide structure (lengths and thicknesses of the semiconducting film in the active and passive waveguides) and show that SPP generation is possible in terahertz range. Such plasmon generators, combining the miniature dimensions and the wideband tunability via variation of geometry parameters, will be especially important for future optoelectronic processors.

Conflict of Interest

The authors declare no conflict of interest.

[1] J. Y. Suh, C. H. Kim, W. Zhou, M. D. Huntington, D. T. Co, M. R. Wasielewski, T. W. Odom, *Nano Lett.* **2012**, *12*, 5769.
[2] D. Y. Fedyanin, *Opt. Lett.* **2012**, *37*, 404.
[3] M. A. Noginov, G. Zhu, A. M. Belgrave, R. Bakker, V. M. Shalaev, E. E. Narimanov, S. Stout, E. Herz, T. Suteewong, U. Wiesner, *Nature* **2009**, *460*, 1110.
[4] I. De Leon, P. Berini, *Nat. Photonics* **2010**, *4*, 382.
[5] J. Seidel, S. Grafström, L. Eng, *Phys. Rev. Lett.* **2005**, *94*, 177401.
[6] M. A. Noginov, G. Zhu, M. Mayy, B. A. Ritzo, N. Noginova, V. A. Podolskiy, *Phys. Rev. Lett.* **2008**, *101*, 226806.
[7] D. Li, M. I. Stockman, *Phys. Rev. Lett.* **2013**, *110*, 106803.
[8] M. Stockman, *Nat. Phys.* **2014**, *10*, 799.
[9] H. P. Paudel, V. Apalkov, M. I. Stockman, *Phys. Rev. B* **2016**, *93*, 155105.
[10] V. Apalkov, M. I. Stockman, *Light Sci. Appl.* **2014**, *3*, 1.
[11] D. A. Svintsov, A. V. Arsenin, D. Y. Fedyanin, *Opt. Express* **2015**, *23*, 19358.
[12] B. Liu, W. Zhu, S. D. Gunapala, M. I. Stockman, M. Premaratne, *ACS Nano* **2017**, *11*, 12573.
[13] Y. S. Dadoenkova, S. G. Moiseev, A. S. Abramov, A. S. Kadochkin, A. A. Fotiadi, I. O. Zolotovskii, *Ann. Phys.* **2017**, *529*, 1700037.
[14] A. S. Kadochkin, S. G. Moiseev, Y. S. Dadoenkova, V. V. Svetukhin, I. O. Zolotovskii, *Opt. Express* **2017**, *25*, 27165.
[15] T. A. Morgado, M. G. Silveirinha, *Phys. Rev. Lett.* **2017**, *119*, 133901.
[16] A. S. Abramov, I. O. Zolotovskii, S. G. Moiseev, D. I. Sementsov, *Quantum Electron.* **2018**, *48*, 22.
[17] I. O. Zolotovskii, Y. S. Dadoenkova, S. G. Moiseev, A. S. Kadochkin, V. V. Svetukhin, A. A. Fotiadi, *Phys. Rev. A* **2018**, *97*, 53828.

[18] P. A. D. Gonçalves, N. M. R. Peres, *An Introduction to Graphene Plasmonics*, World Scientific Publishing Co. Pte. Ltd., Singapore **2016**.

[19] V. M. Agranovich, D. L. Mills (eds.), *Surface Polaritons*, North-Holland, Amsterdam **1982**.

[20] H. Raether, *Surface Plasmons on Smooth and Rough Surfaces and on Gratings*, Springer, Berlin/Heidelberg, Germany **1988**.

[21] D. I. Trubetskov, A. E. Khramov, *Lectures on Microwave Electronics for Physicists*, Fizmatlit, Moscow **2003**.

[22] S. E. Tsimring, *Electron Beams and Microwave Vacuum Electronics*, Wiley, New York **2006**.

[23] J. Pierce, *Electrons and Waves*, Anchor Books, New York **1964**.

[24] E. D. Palik, *Handbook of Optical Constants of Solids*, Academic Press, San Diego, CA, USA **1998**.

[25] G. W. Hanson, *J. Appl. Phys.* **2008**, *103*, 064302.

[26] V. P. Gusynin, S. G. Sharapov, J. P. Carbotte, *J. Phys. Condens. Matter* **2007**, *19*, 026222.

[27] K. S. Novoselov, A. K. Geim, S. V. Morozov, D. Jiang, M. I. Katsnelson, I. V. Grigorieva, S. V. Dubonos, A. A. Firsov, *Nature* **2005**, *438*, 197.

[28] M. D. Ozdemir, O. Atasever, B. Ozdemir, Z. Yarar, M. Ozdemir, *AIP Adv.* **2015**, *5*, 077101.

[29] M. A. Yamoah, W. Yang, E. Pop, D. Goldhaber-Gordon, *ACS Nano* **2017**, *11*, 9914.

[30] H. Ramamoorthy, R. Somphonsane, J. Radice, G. He, C.-P. Kwan, J. P. Bird, *Nano Lett.* **2016**, *16*, 399.

[31] C. Hwang, D. A. Siegel, S.-K. Mo, W. Regan, A. Ismach, Y. Zhang, A. Zettl, A. Lanzara, *Sci. Rep.* **2012**, *2*, 590.

[32] P. V. Ratnikov, A. P. Silin, *JETP Lett.* **2014**, *100*, 311.

[33] D. C. Elias, R. V. Gorbachev, A. S. Mayorov, S. V. Morozov, A. A. Zhukov, P. Blake, L. A. Ponomarenko, I. V. Grigorieva, K. S. Novoselov, F. Guinea, A. K. Geim, *Nat. Phys.* **2011**, *7*, 701.

[34] Z. Q. Li, E. A. Henriksen, Z. Jiang, Z. Hao, M. C. Martin, P. Kim, H. L. Stormer, D. N. Basov, *Nat. Phys.* **2008**, *4*, 532.

[35] G. Li, A. Luican, E. Y. Andrei, *Phys. Rev. Lett.* **2009**, *102*, 176804.

[36] A. Yariv, *Quantum Electronics*, 3rd ed., Wiley, New York **1989**.

[37] R. Zia, A. Chandran, M. L. Brongersma, *Opt. Lett.* **2005**, *30*, 1473.

[38] J. Moreland, A. Adams, P. K. Hansma, *Phys. Rev. B*, **1982**, *25*, 2297.

[39] D. Choi, I. Lee, J. Jung, J. Park, J.-H. Han, B. Lee, *J. Lightwave Technol.* **2009**, *27*, 5675.

[40] P. T. Worthing, W. L. Barnes, *Appl. Phys. Lett.* **2001**, *79*, 3035.